

Bounds on charging power of open quantum batteries

S. Zakavati,^{1,*} F. T. Tabesh,^{1,*} and S. Salimi^{1,†}

¹*Department of Physics, University of Kurdistan, P.O.Box 66177-15175, Sanandaj, Iran*

(Dated: December 22, 2024)

In general, quantum systems most likely undergo open system dynamics due to their smallness and sensitivity. Energy storage devices, so-called quantum batteries, are not excepted from this phenomenon. Here, we study fundamental bounds on the power of open quantum batteries from the geometric point of view. By defining an *activity operator*, a tight upper bound on the charging power is derived for the open quantum batteries in terms of the fluctuations of the activity operator and the quantum Fisher information. The variance of the activity operator may be interpreted as a generalized thermodynamic force, while the quantum Fisher information describes the speed of evolution in the state space of the battery. The thermodynamic interpretation of the upper bound is discussed in detail. As an example, a model for the battery, taking into account the environmental effects, is proposed and the effect of dissipation and decoherence during the charging process on both the stored work and the charging power is investigated. Our results show that the upper bound is saturated in some time intervals. Also, the maximum value of both the stored work and the corresponding power is achieved under the non-Markovian dynamics and underdamped regime.

PACS numbers: 03.65.Yz, 42.50.Lc, 03.65.Ud, 05.30.Rt

I. INTRODUCTION

Recently, there has been a great deal of interest in studying quantum thermodynamics by increasing requests for device miniaturization [1–3]. The study of thermodynamic concepts in a quantum context is of great importance, both from a fundamental and a practical point of view [4–7]. One of the main purposes of these blossoming researches is to propose various mechanisms to store and transfer energy beyond the microscopic scale. Hence, Quantum batteries (*QBs*) are introduced as finite dimensional quantum devices that are able to temporarily store energy in quantum degrees of freedom and transfer the energy to other apparatus [8–16]. *QBs* have yet been suggested in a number of models, such as spin systems [17], quantum cavities [9, 11, 18], superconducting transmon qubits [19], Josephson quantum phase battery [20], molecular battery [21], Sachdev-Ye-Kitaev model [22], and quantum oscillators [14, 23].

In most literature, *QBs* are regarded as closed systems which follow entirely the unitary evolution. However, due to the fragile nature of all quantum systems, it sounds plausible that batteries may interact with the surrounding environment, leading to the dissipation of the stored energy. To deal with this issue, the concept of open quantum batteries (*OQBs*) has been introduced in recent years [24–33]. The evolution of *OQBs* can be characterized by means of a family of completely positive and trace-preserving maps. Consequently, *OQBs* dynamics can be either Markovian or non-Markovian [34–36]. The interaction of the *OQBs* with their reservoirs can lead to energy dissipation and decoherence. Hence, it is essential to find strategies to stabilize the energy storage against energy leakage into an environment [24, 25, 30, 31]. To suppress these unwanted effects, recent research efforts

have been devoted to retaining energy with no dissipation in *OQBs* [24–31].

In the case of *QBs*, charging is a procedure during which the state of a system is transferred from lower to higher energy levels. In general, the *QB* charging protocol is composed of a *QB* and a charger (energy source), where energy flows from the charger into the battery by establishing an interaction between them. In order to study the thermodynamic behaviour of the charging and the reverse process known as work extraction, in the context of quantum thermodynamics, the main objective is to derive a consistent formulation for the desired thermodynamic quantities from the established quantum principles. One of the well-known and essential principles in quantum theory is Heisenberg’s uncertainty relation. In its practical statement, the uncertainty relation is interpreted as setting a fundamental bound on the intrinsic time scale of any quantum evolution. In other words, time-energy uncertainty quantifies how fast a quantum system can evolve. *QB* Hamiltonian quantifies the amount of energy that can be deposited in the battery. Due to the fact that battery Hamiltonian has finite magnitude, it holds a fundamental bound on the minimum time required to transform a given initial state to a given final state. Minimizing the charging time and maximizing the associated power are figures of merit in *QBs*. In the framework of quantum speed limit (*QSL*) and geometry of quantum space, minimized evolution time is obtained when the dynamical trajectory reaches to the *geodesic* path. The *geodesic* path denotes the shortest length among all physical evolution trajectories between the given initial and final states. As the space of quantum states equipped with the proper metric, the *geodesic* distance can be calculated. Here, we will be working with the Bures metric in which the corresponding *geodesic* distance is known.

So far, two different bounds have been introduced for the charging power. The first one proposed by Farré et al. [37], by means of a quantum geometrical approach, a bound was derived in terms of the energy variance of the battery and the Fisher information in the eigenspace of the battery Hamil-

*These authors contributed equally to this work.

†Electronic address: ShSalimi@uok.ac.ir

tonian for closed QBs . In another study conducted by Pintos et al.[33], the bound was defined in terms of the interaction Hamiltonian fluctuations and *work operator* fluctuations. The later was shown to be valid for closed QBs as well as $OQBs$. Also, they concluded that there must exist fluctuations in the extractable work stored in the battery to have a non-zero charging power.

Motivated by the above considerations and recent progress in $OQBs$, this study aims to answer the following questions: Is it possible to generalize a bound on the charging power for $OQBs$ in the context of the geometry of quantum states? if so, what is the thermodynamic description of terms appear in this bound? Can one engineer a dissipative charging process for a battery and keep the stored energy stabilized by using quantum memory effects? To address the questions, we study bounds on the charging power and generalize the previous bounds. Due to the fact that every system out of equilibrium in contact with a thermal bath contains an amount of free energy that can do work, we define an *activity operator* which quantifies how far the state of the system distances from equilibrium. A tight upper bound on charging power in terms of quantum Fisher information (QFI) and the variance of the activity operator of $OQBs$ is proved. By dividing the dissipation part of Lindblad master equation into a diagonal part and a non-diagonal part, a redefinition for the bound in terms of dissipative work and entropy production rate is proposed. Moreover, the role of dissipation effects and the backflow of information on the stored work and charging power is explored. For this, an example will be considered in which a battery interacts with dissipative and heating reservoirs at finite temperature. We will show that the stored work and the power are maximal for both non-Markovian dynamics and underdamped regime. Results indicate that the charging power of OQB can boost by increasing temperature if interaction parameters, coupling coefficient, and temperature are adjusted properly. despite the fact that one may anticipate the performance of QBs can be spoiled at high temperatures.

The paper is organized as follows. In Sec. II bounds on the charging power of open systems are provided. The derivations in Sec. III. sheds light on the Thermodynamics interpretation of the bound. In sec. IV, a more physically upper bound on the charging power is suggested based on an extended QFI. In order to illustrate the upper bound is tight, Heisenberg XX spin chain example is presented in Sec. V. Also, a heuristic model of OQB is investigated in the presence of a bath. The conclusion is summarized in Sec. VI.

II. BOUNDS ON CHARGING POWER

First, a general model describing $OQBs$ is presented. The model is constructed from a quantum system as a battery and a charging protocol. The battery system also interacts with a thermal bath in the framework of open system analysis. The Hamiltonian of the whole system of the charger A , the battery B and the bath E is defined by

$$H = H_A + H_B + H_E + H_{int}, \quad (1)$$

where H_A , H_B and H_E are the charger, the battery and the bath free Hamiltonians, respectively. H_{int} includes all interactions with the QB . Note that, H_B is time independent. Therefore, in the interaction picture, the reduced density matrix of the QB at time t can be written as

$$\partial_t \rho = -i \text{Tr}_{(AE)}[H_{int}, \rho]. \quad (2)$$

For a system in contact with a thermal bath, every state of the system out of equilibrium contains an amount of free energy that can be extracted in the form of work. The non-equilibrium free energy is defined as

$$F(\rho) = U - \beta^{-1} S(\rho), \quad (3)$$

in which, $U = \text{Tr}(\rho H_s)$ and $S(\rho) = -\text{Tr}(\rho \ln \rho)$ denote the energy and von Neumann entropy of the system, [38–40] respectively. In the relaxation process, the free energy of the system naturally tends to decrease until it reaches its minimum value. The equilibrium state, therefore, denotes the state at which the free energy minimized. By assuming that the instantaneous state of the QB is ρ , and the thermal equilibrium state is indicated by $\tau_\beta = \frac{1}{Z} \exp(-\beta H_B)$ where $Z = \text{Tr}(\exp(-\beta H_s))$ is the partition function, The Maximum extractable work from the battery system is given by

$$W_{max} = F(\rho) - F(\tau_\beta), \quad (4)$$

In the following, by defining $\mathcal{A} := \beta^{-1} \log \left(\frac{\rho}{\tau_\beta} \right)$ as the *activity operator*, we can rewrite the maximum extractable work as

$$W_{max} = \frac{1}{\beta} \text{Tr}(\rho (\ln \rho - \ln \tau_\beta)) = \text{Tr}(\rho \mathcal{A}). \quad (5)$$

When the system is at equilibrium, obviously, $\mathcal{A} = 0$ and $\mathcal{A} > 0$ for any other non-equilibrium state. The activity operator quantifies how far the state of the system distances from equilibrium. In other words, activity operator associated with a state of the system indicates how much the state is *active* or has an availability to extract work from it.

In [33], $\mathbb{F} = H_B + \beta^{-1} \log \rho$ has been introduced as *work operator*.

How fast the work can stored on the QB depends on its charging power, i.e., the rate at which the energy flows in the QB during the interaction. The charging power is determined by

$$\frac{d}{dt}(W_{max}) = \frac{d}{dt} \text{Tr}(\rho \mathcal{A}) = \text{Tr}(\dot{\rho} \mathcal{A}), \quad (6)$$

as a result,

$$\mathbb{P} = \text{Tr}(\dot{\rho} \mathcal{A}). \quad (7)$$

Now, based on the above formula, an upper bound for charging power of a OQB is found. As mentioned earlier, the upper bound on the power saturates when the time required to transform a given initial state to a given final state is minimized. It occurs when among all the possible dynamical trajectories,

the system evolves through the geodesic path, which is the shortest curve between two distinguishable states. The distinguishability of quantum states can be measured by a distance measure on density operator space. In this case, we consider Bures angle, which has the advantage that whose geodesic is analytically known and equivalent to quantum fisher information metric. A well-known statement for the QFI can be provided by the use of symmetric logarithmic derivative

$$I_Q(\diamond) = \text{Tr}(\rho L(\diamond)^2), \quad (8)$$

in which, \diamond denotes the desired parameter and the Hermitian operator L for a given state $\rho(t)$ and t as a parameter is defined through [41]

$$\partial_t \rho = \frac{1}{2}(L \rho + \rho L). \quad (9)$$

Note that hereafter, the parameter dependence is omitted to simplify the notation. By replacing the above formula in Eq. (8) and by defining $\delta \mathcal{A} = \mathcal{A} - \langle \mathcal{A} \rangle$, one can obtain

$$\begin{aligned} |\mathbb{P}| &= |\text{Tr}(\frac{1}{2}(L \rho + \rho L^\dagger) \delta \mathcal{A})| \\ &\leq \frac{1}{2}|\text{Tr}(L \rho \delta \mathcal{A})| + \frac{1}{2}|\text{Tr}(\rho L \delta \mathcal{A})|. \end{aligned} \quad (10)$$

By employing the Cauchy-Schwarz inequality on the right-hand side of Eq. (10), one can obtain the following inequality

$$|\mathbb{P}| \leq \sigma_{\mathcal{A}} \sqrt{I_Q}, \quad (11)$$

where $\sigma_{\mathcal{A}}^2 = \langle \mathcal{A}^2 \rangle - \langle \mathcal{A} \rangle^2$ is the standard deviations of the activity operator. The above inequality shows an upper bound on the charging power, which generalizes the bound proposed for closed QBs [37] to OQB s. Note that the square root of the quantum Fisher information represents the speed of evolution in the state space of the battery. Therefore, an immediate insight from Eq. 11 reminds us of the familiar formula of power in classical physics $P = F.v$, where F can be any (constant) force and V is the flow velocity relative to the object. therefore, In comparison with this formula, the variance of the activity operator may be characterized as generalized thermodynamic force. The activity operator associated with a non-equilibrium state, therefore, drives the system towards the equilibrium state. A similar statement for the thermodynamic force provided in [42]. It is expected that At equilibrium, \mathcal{A} as all thermodynamic forces must vanish. An example to further clarify this phenomenon is the temperature gradient which can be regarded as a thermodynamic force that causes an irreversible flow of heat between to systems until they reach the same temperature.

In the next section by using the Lindblad type master equation, we obtain thermodynamic interpretation of the upper bound in terms of the dissipative work and the entropy production rate.

III. THERMODYNAMIC INTERPRETATION OF THE BOUND

Having introduced the model of OQB and a definition for power, we explain the bound in terms of thermodynamic con-

cepts such as work and entropy production. To this aim, By taking the partial trace over the bath and charger in Eq. (2), the reduced dynamics of the QB can be described by the following master equation [34]

$$\partial_t \rho = -i [H_B(t), \rho(t)] + D[\rho(t)], \quad (12)$$

where the first term represents the unitary part of the dynamics. The term $D[\rho(t)]$ represents the quantum dissipater which is defined as

$$D[\rho(t)] = \sum_{\alpha} \gamma_{\alpha}(t) [L_{\alpha} \rho(t) L_{\alpha}^{\dagger} - \frac{1}{2} \{L_{\alpha}^{\dagger} L_{\alpha}, \rho(t)\}], \quad (13)$$

in which L_{α} and $\gamma_{\alpha}(t)$ are Lindblad operators and decay rates, respectively.

In the following, by considering the spectral decomposition of the density matrix, i.e., $\rho(t) = \sum_n P_n(t) |n(t)\rangle \langle n(t)|$, the dissipater can be split as [43]

$$D[\rho(t)] = D_d[\rho] + D_{nd}[\rho], \quad (14)$$

where the diagonal part is

$$\begin{aligned} D_d[\rho] &= \sum_n \langle n | D[\rho] | n \rangle | n \rangle \langle n | \\ &= \sum_n \partial_t P_n | n \rangle \langle n | = - \{ \Gamma(t), \rho(t) \}, \end{aligned} \quad (15)$$

in which, $\Gamma(t)$ is defined as

$$\Gamma(t) = -\frac{1}{2} \sum_n \frac{\partial_t P_n}{P_n} | n \rangle \langle n |, \quad (16)$$

as suggested in [45]. The non-diagonal part of the dissipater can be written as

$$D_{nd}[\rho] = \sum_{n \neq m} \langle n | D[\rho(t)] | m \rangle | n \rangle \langle m |. \quad (17)$$

By introducing the dissipative Hamiltonian

$$H_{Diss}(t) = \sum_{n \neq m} \frac{-i \langle n | D[\rho] | m \rangle}{P_m - P_n} | n \rangle \langle m |, \quad (18)$$

thus, Eq. (17) takes the following form

$$D_{nd}[\rho] = -i [H_{Diss}(t), \rho(t)]. \quad (19)$$

The above relation can be expounded as part of the bath dynamics which generates a unitary time-evolution [43].

As a result, the Lindblad master equation can be written as

$$\partial_t \rho = -i [\tilde{H}, \rho(t)] - \{ \Gamma(t), \rho(t) \}, \quad (20)$$

where $\tilde{H} = H(t) + H_{Diss}(t)$.

In the following, substituting the Eq. (20) into Eq. (7), one can find

$$\begin{aligned} |\mathbb{P}| &= |\text{Tr}(-i [\tilde{H}, \rho] \mathcal{A}) + \text{Tr}(- \{ \Gamma(t), \rho \} \mathcal{A})| \\ &\leq |\text{Tr}(-i [\tilde{H}, \rho] \mathcal{A})| + |\text{Tr}(- \{ \Gamma(t), \rho \} \mathcal{A})|. \end{aligned} \quad (21)$$

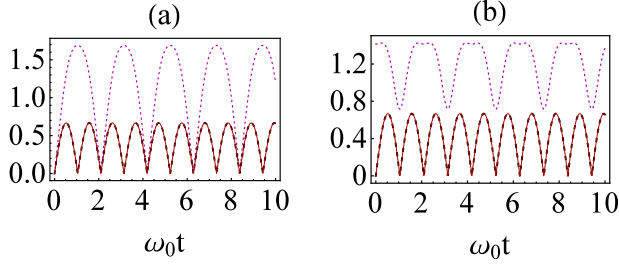


FIG. 1: (Color online). Plot of $(2\sigma_V \sigma_F)/\omega_0$ (dotted magenta line) and $(\sigma_A \sqrt{I_Q})/\omega_0$ (dashed black line) and $|\mathbb{P}|/\omega_0$ (red solid line) as a function of $\omega_0 t$. We have used $\alpha = 0$, $\beta = 0$, and $\gamma = 1$ in (a) and $\alpha = 0$, $\beta = 1/\sqrt{2}$, and $\gamma = 1/\sqrt{2}$ in (b). Other parameters are $J = \omega_0$, and $B = 0$.

Considering $\mathcal{A} = H_B + \beta^{-1} \log \rho + F_{\tau_\beta}$, one can obtain

$$|\mathbb{P}| \leq \left| \text{Tr}([\rho, \tilde{H}] H_B) \right| + \left| \text{Tr} \left(\sum_n \dot{P}_n |n\rangle \langle n| (H_B + \beta^{-1} \log \rho) \right) \right|. \quad (22)$$

The first term in the right-hand side of Eq. (22) can be regarded as

$$\begin{aligned} \left| \text{Tr}([\rho, \tilde{H}] H_B) \right| &= \left| \text{Tr}([\rho, H_B + H_{Diss}] H_B) \right| \\ &= \left| \text{Tr}([\rho, H_{Diss}] H_B) \right| = W_{Diss}, \end{aligned} \quad (23)$$

and the second sentence presents the change in the irreversible entropy S_{irr} , can be taken as [46, 47]

$$\begin{aligned} \left| \text{Tr} \left(\sum_n \dot{P}_n |n\rangle \langle n| (\beta^{-1} \log \rho) \right) + \text{Tr} \left(\sum_n \dot{P}_n |n\rangle \langle n| H_B \right) \right| \\ = \left| -\frac{1}{\beta} dS + dQ \right| = \frac{1}{\beta} |dS_{irr}|. \end{aligned} \quad (24)$$

Therefore, combining the equations (22), (23) and (24), the charging power is bounded from above as the following form

$$|\mathbb{P}| \leq W_{Diss} + \frac{1}{\beta} |dS_{irr}|. \quad (25)$$

In the next section, the upper bound in Eq. (11) will be illustrated by means of a Heisenberg XX spin chain for three qubits, and quantum battery in dissipation/heating reservoir. We will see that the bound in Eq. (11) is saturated with these cases. In addition, we will study the role of non-Markovian effects on energy conservation and enhance of charging power.

IV. DERIVATION OF THE UPPER BOUND: EXTENDED QFI

In Sec. II, the standard QFI was employed to derive an upper bound on charging power. Furthermore, splitting the

dissipater into dissipative (non-unitary) and coherent (unitary) contributions allows one to write the whole master equation as commutator and anti-commutator parts, which is valid for the Lindblad-like master equations. By considering the time as a parameter, such a decomposition of quantum Liouvillian has been based to introduce an extended QFI in terms of the non-Hermitian SLD [44, 45]. The extended QFI is defined as an upper bound on the QFI.

$$I_Q(x) \leq \text{Tr} \left[\tilde{L}(x) \rho \tilde{L}(x)^\dagger \right], \quad (26)$$

in which, the nSLD \tilde{L} satisfies $\partial_x \rho = \left(\tilde{L}(x) \rho + \rho \tilde{L}(x)^\dagger \right) / 2$. The right-hand side of the above inequality denoted by I_Q^{ext} . Considering Eq. (20) and t as the parameter, nSLD reads

$$\tilde{L} = -2i(\tilde{H} - i\Gamma(t)). \quad (27)$$

In the following, by the similar procedure as in sec. II, a bound on charging power in terms of the extended QFI is obtained

$$P(t) \leq |\text{Tr}[\dot{\rho} \mathcal{A}]| = \left| \text{Tr} \left[\frac{(\tilde{L} \rho + \rho \tilde{L}^\dagger)}{2} \right] \delta \mathcal{A} \right|. \quad (28)$$

The triangle and the Cauchy-Schwarz inequalities imply that

$$\begin{aligned} P(t) &\leq \frac{1}{2} |\text{Tr}(\tilde{L} \rho \delta \mathcal{A})| + \frac{1}{2} \left| \text{Tr}(\rho \tilde{L}^\dagger \delta \mathcal{A}) \right| \\ &= \frac{1}{2} |\text{Tr}(\sqrt{\rho} \delta \mathcal{A} \tilde{L} \sqrt{\rho})| + \frac{1}{2} \left| \text{Tr}(\sqrt{\rho} \tilde{L}^\dagger \delta \mathcal{A} \sqrt{\rho}) \right| \\ &\leq 2 \times \frac{1}{2} \sqrt{\text{Tr}(\tilde{L} \rho \tilde{L}^\dagger) \text{Tr}(\rho \delta \mathcal{A}^2)} = \sqrt{I_Q^{ext} \sigma_{\mathcal{A}}}. \end{aligned} \quad (29)$$

In the above equation, the square root of I_Q^{ext} can be interpreted as the speed of evolution. Here, we are interested to separate this velocity term into contributions with certain physical interpretation. Substituting Eq.(27) in the interaction picture) into I_Q^{ext} gives

$$\begin{aligned} I_Q^{ext} &= 4 \text{Tr} \left((\tilde{H} - i\Gamma(t)) \rho (H_{Diss} + i\Gamma(t)) \right) \\ &= \text{Tr} \left(\rho \left(H_{Diss}^2 + \sum_n \left[\frac{\partial_t P_n}{P_n} \right]^2 |n\rangle \langle n| \right) \right), \end{aligned} \quad (30)$$

where in the second line we also have used Eq. (16). Here, One can show that the $\text{Tr}(\rho (H_{Diss})) = 0$, therefore, the first term in the second line implies the variance of the H_{Diss} . By using of the spectral decomposition of the density matrix, we can conclude

$$I_Q^{ext} = \sigma_{H_{Diss}}^2 + \sum_n \left[\frac{\partial_t P_n^2}{P_n} \right]. \quad (31)$$

The second term clearly represents the classical Fisher information. Thus, the fluctuations of the dissipative work denotes the pure quantum part of the extended QFI. This sounds

sensible since the Hamiltonian of H_{Diss} results from off-diagonal(coherent) part of dissipater. Note that The square root of QFI can be understood as the velocity at which system is transmitted between initial and final state. Therefore

$$\sqrt{I_Q^{ext}} = v(t) = \sqrt{v_{CL}(t)^2 + v_Q(t)^2}. \quad (32)$$

As a conclusion, Eq. (32) separates the speed of evolution into a classical and a quantum contribution. Each part relates to a physically meaningful quantity. In other words, the individual role of populations of the state and the coherences in driving the evolution is clarified.

V. EXAMPLES

A. The Heisenberg XX spin chain

As the first example, we consider the three-qubit Heisenberg XX spin chain that the second qubit is regarded as the system and other qubits as the environment. The free Hamiltonian is

$$H_0 = \frac{\omega_0}{2} \left(\sum_{n=1}^3 \sigma_n^z + 1_n \right), \quad (33)$$

where ω_0 is the transition frequency of each of qubits and for the sake of convenience, we assume ground-state energy is zero. The interaction Hamiltonian characterizing the chain exposed to a uniform magnetic field is given by

$$V = \frac{J}{2} \sum_{n=1}^3 (\sigma_n^x \sigma_{n+1}^x + \sigma_n^y \sigma_{n+1}^y) + B \sum_{n=1}^3 \sigma_n^z, \quad (34)$$

where σ_n^α displays the Pauli operator corresponding to each α ($\alpha = x, y, z$), J marks the exchange interaction constant, and B is the magnitude of a uniform magnetic field [48]. Suppose the periodic boundary conditions, $\sigma_1^x = \sigma_4^x$ and $\sigma_1^y = \sigma_4^y$, and considering eigenvalues and eigenstates of the Hamiltonian, if we assume the normalized initial state as

$$|\Psi(0)\rangle = \alpha|001\rangle + \beta|010\rangle + \gamma|100\rangle, \quad (35)$$

its time evolution will be

$$|\Psi(t)\rangle = a(t)|001\rangle + b(t)|010\rangle + c(t)|100\rangle, \quad (36)$$

where

$$\begin{aligned} a(t) &= \frac{1}{3}(e^{it(J+B)}(2\alpha - \beta - \gamma) + K(t)), \\ b(t) &= \frac{1}{3}(e^{it(J+B)}(2\beta - \alpha - \gamma) + K(t)), \\ c(t) &= \frac{1}{3}(e^{it(J+B)}(2\gamma - \alpha - \beta) + K(t)), \end{aligned} \quad (37)$$

in which $K(t) = e^{-it(2J-B)}(\alpha + \beta + \gamma)$.

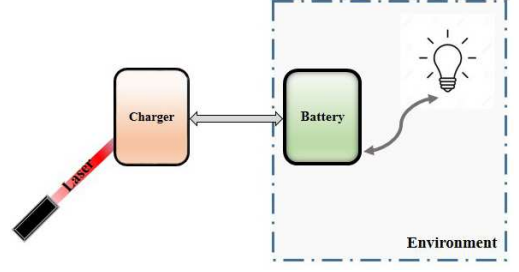


FIG. 2: Schematic diagrams of an open QB . A quantum battery interacts with a charger during the charging process, while the battery is coupled individually into an environment. In addition, an external field is applied to the charger.

Here, if we consider $\rho = \sum_{\lambda_i \in S} \lambda_i |\lambda_i\rangle \langle \lambda_i|$, where $S = \{\lambda_i \in \{\lambda_i\} | \lambda_i \neq 0\}$ is the support, the quantum Fisher information for the parameter t can be calculated as [49]

$$\begin{aligned} I_Q &= \sum_{\lambda_i \in S} \frac{(\partial_t \lambda_i)^2}{\lambda_i} + \sum_{\lambda_i \in S} 4\lambda_i \langle \partial_t \lambda_i | \partial_t \lambda_i \rangle \\ &\quad - \sum_{\lambda_i, \lambda_j \in S} \frac{8\lambda_i \lambda_j}{\lambda_i + \lambda_j} |\langle \partial_t \lambda_i | \lambda_j \rangle|^2. \end{aligned} \quad (38)$$

Using Eqs. (6), (33), (36) and the above equation, one can obtain the following equality

$$|\mathbb{P}| = \sqrt{I_Q} \sigma_{\mathcal{A}} = \omega_0 |\dot{b}b^* + b\dot{b}^*|, \quad (39)$$

we see that the equality sign in Eq. (39) holds where displays the upper bound is saturated with this case. For comparison with the bound in Ref. [33], we have plotted the upper bounds and $|\mathbb{P}|$ in Fig. 1 as a function of $\omega_0 t$, where dotted magenta line represents $(2\sigma_V \sigma_{\mathbb{F}})/\omega_0$, dashed black line shows $(\sigma_{\mathcal{A}} \sqrt{I_Q})/\omega_0$ and red solid lines indicate $|\mathbb{P}|/\omega_0$. We have $\alpha = 0, \beta = 0, \gamma = 1$ in Fig. 1(a) and $\alpha = 0, \beta = 1/\sqrt{2}, \gamma = 1/\sqrt{2}$ in Fig. 1(b). As can be seen $\sigma_{\mathcal{A}} \sqrt{I_Q}$ is reached while $2\sigma_V \sigma_{\mathbb{F}}$ is greater than $|\mathbb{P}|$.

B. Quantum battery and dissipative/heating reservoir

Here, we assume a charging protocol where the QB is immersed in a reservoir including the effects of dissipation and heating see Fig. 2. Let us consider the case in which both the charger A and the QB are two qubits. The total Hamiltonian is expressed as [32]

$$H = H_0 + \Delta H_A + H_{AB} + H_{BE}, \quad (40)$$

where the first term is the free Hamiltonian of the total system, that it is given by

$$H_0 = \frac{\omega_0}{2} (\sigma_z^A + 1) + \frac{\omega_0}{2} (\sigma_z^B + 1) + \sum_k \omega_k b_k^\dagger b_k, \quad (41)$$

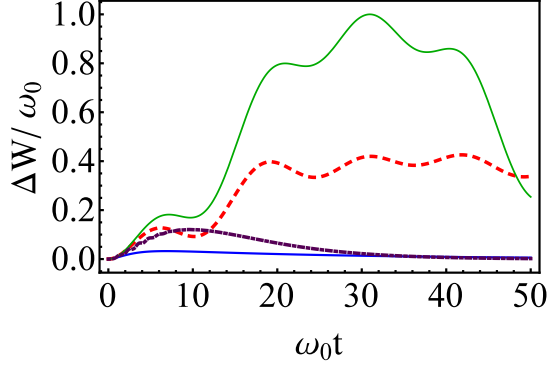


FIG. 3: (Color online). Plot of $\Delta W/\omega_0$, (in units of ω_0), as a function of $\omega_0 t$. Numerical results in this plot have been obtained by setting $\eta = 0.1\omega_0$, $\Delta = 3\omega_0$ and $T = 0$. Solid blue line (overdamped regime) and dashed red line (underdamped regime) present local markovian dynamics ($R = 0.01$) for $\gamma_0 = \omega_0, \lambda = 100\omega_0$, $\kappa = 0.001\omega_0$ and $\gamma_0 = 0.1\omega_0, \lambda = 10\omega_0$, $\kappa = 0.2\omega_0$, respectively. Dotted purple line (overdamped regime) and solid green line (underdamped regime) remarks local non-Markovian dynamics ($R = 10$) for $\gamma_0 = 10\omega_0, \lambda = 1\omega_0$, $\kappa = 0.001\omega_0$ and $\gamma_0 = 0.1\omega_0, \lambda = 0.01\omega_0$, $\kappa = 0.2\omega_0$, respectively. We have considered $|\varphi_{AB}(0)\rangle = |1\rangle \otimes |0\rangle$.

and interaction Hamiltonians can be

$$\begin{aligned}\Delta H_A &= \eta(\sigma_+^A e^{-i\omega_0 t} + \sigma_-^A e^{i\omega_0 t}), \\ H_{AB} &= \kappa(\sigma_+^A \sigma_-^B + \sigma_-^A \sigma_+^B), \\ H_{BE} &= \sum_k g_k(\sigma_+^B b_k + \sigma_-^B b_k^\dagger),\end{aligned}\quad (42)$$

with $\sigma_\pm^{A,B}$ being the raising and the lowering operators of the corresponding qubit, ω_0 and ω_k the transition frequency of the qubits and the environment, b_k (b_k^\dagger) is the annihilation (creation) operator corresponding to the k th mode of the bosonic environment, g_k indicates the coupling constant between the battery and the k th mode of the environment. The second term in Eq. (41), ΔH_A , defines an external resonant driving field with amplitude η that may inject energy into the system and the third term, H_{AB} , shows the interaction Hamiltonian between the charger and the battery by the coupling constant κ . Finally, H_{BE} describes the interaction between the battery and the bath at temperature T . We emphasize that the charger does not couple to the bath. In the interaction picture representation, the corresponding master equation of the model explicitly reads as [32, 51]

$$\begin{aligned}\frac{d\rho^{AB}}{dt} &= -i[\kappa(\sigma_+^A \sigma_-^B + \sigma_-^A \sigma_+^B) + \eta(\sigma_+^A + \sigma_-^A), \rho^{AB}] \\ &+ \frac{\gamma_1(t)}{2}(\sigma_+^B \rho^{AB} \sigma_-^B - \frac{1}{2}\{\sigma_-^B \sigma_+^B, \rho^{AB}\}) \\ &+ \frac{\gamma_2(t)}{2}(\sigma_-^B \rho^{AB} \sigma_+^B - \frac{1}{2}\{\sigma_+^B \sigma_-^B, \rho^{AB}\}),\end{aligned}\quad (43)$$

where $\gamma_{1,2}$ shows time-dependent decay rates that the second and third terms describe heating and dissipation, respectively.

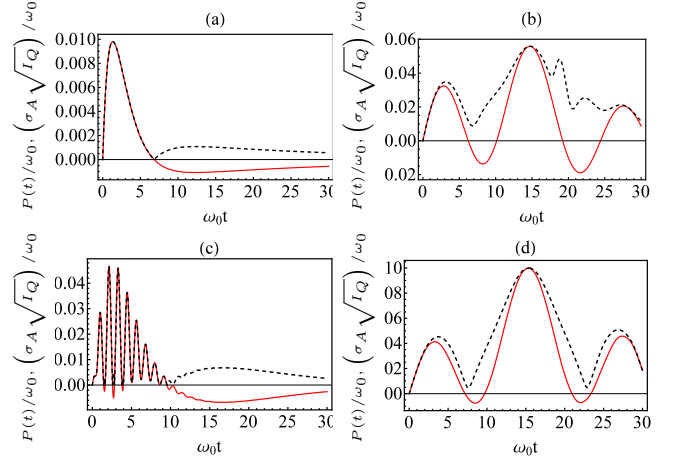


FIG. 4: (Color online). Plot of $\sigma_A \sqrt{I_Q}$ (dashed black line) and \mathbb{P} (red solid line) (in units of ω_0) as a function of $\omega_0 t$ for $T = 0$. Local Markovian dynamics for overdamped and underdamped regime is shown in (a) and (b), respectively. Also, local non-Markovian dynamics for overdamped and underdamped regime is illustrated in (c) and (d), respectively. The parameters are the same as Fig. 3

Suppose the spectral density of the environment is taken as

$$J(\omega) = \gamma_0 \lambda^2 / 2\pi [(\omega_0 - \Delta - \omega)^2 + \lambda^2], \quad (44)$$

in which γ_0 is an effective coupling constant related to the relaxation time of the battery $\tau_R \approx 1/\gamma_0$ and the width of the spectrum is presented by λ connected to the reservoir correlation time $\tau_B \approx 1/\lambda$. Also, $\Delta = \omega_0 - \nu_c$ is the detuning and ν_c is the central frequency of the thermal reservoir [34]. By taking into account these considerations, the decay rates are given by $\gamma_1(t)/2 = (N)f(t)$ and $\gamma_2(t)/2 = (N+1)f(t)$, where $N = 1/[\exp(\omega_0/K_B T) - 1]$ represents the mean number of photons in the modes of the thermal reservoir at temperature T and the function $f(t)$ depends on the form of the reservoir spectral density. Moreover, notice that the heating rate vanishes at zero temperature, i.e., $\gamma_1(t) = 0$, and the dissipation rate is determined by $\gamma_2(t)/2 = f(t)$ [34]. The function $f(t)$ obtained in the exactly solvable form and it is given by [34]

$$\begin{aligned}f(t) &= -2\Re\left\{\frac{\dot{C}(t)}{C(t)}\right\}, \\ C(t) &= e^{-(\lambda - i\Delta)t/2} \left(\cosh\left(\frac{dt}{2}\right) + \frac{\lambda - i\Delta}{d} \sinh\left(\frac{dt}{2}\right) \right) C(0),\end{aligned}\quad (45)$$

with $d = \sqrt{(\lambda - i\Delta)^2 - 2\gamma_0\lambda}$. We can also define $R = \gamma_0/\lambda$ in order to distinguish the strong coupling regime from the weak coupling regime. It has been demonstrated that in the strong coupling regime, $R \gg 1$, the function $f(t)$ might take on negative values within certain time intervals, hence the dynamics of the qubit becomes nondivisible and non-Markovian [36, 50]. In order to solve Eq. (43), we write ρ^{AB} in the

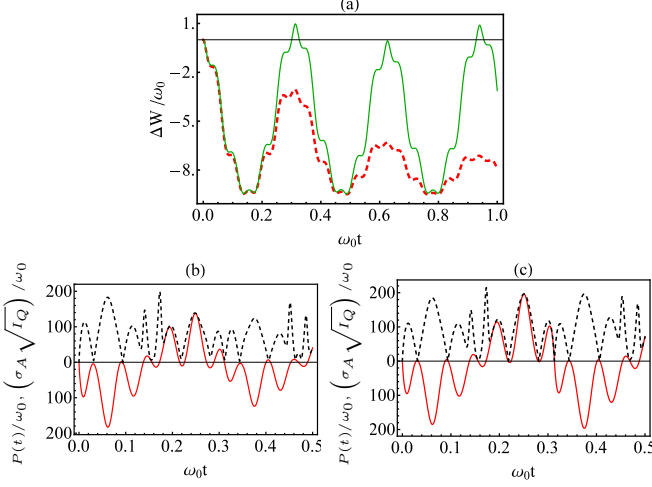


FIG. 5: Plane (a) shows ΔW for underdamped regime, where solid green line and dashed red line show non-Markovian and Markovian dynamics, respectively. Planes (b) and (c) illustrate $\sigma_{\mathcal{A}} \sqrt{I_Q}$ (dashed black line) and \mathbb{P} (solid red line), in units of ω_0 , as a function of $\omega_0 t$ for Markovian and non-Markovian dynamics, respectively. We have used $N = 5$, $K_B T = 10\omega_0$, $\eta = 10\omega_0$ and $\kappa = 50\omega_0$. Other parameters are as Fig.3.

matrix form

$$\rho_{AB}(t) = \begin{pmatrix} r_{11}(t) & r_{12}(t) & r_{13}(t) & r_{14}(t) \\ r_{21}(t) & r_{22}(t) & r_{23}(t) & r_{24}(t) \\ r_{31}(t) & r_{32}(t) & r_{33}(t) & r_{34}(t) \\ r_{41}(t) & r_{42}(t) & r_{43}(t) & r_{44}(t) \end{pmatrix}. \quad (46)$$

Substituting the above matrix into Eq. (43) one can attain a first-order system of ordinary differential equations in the sixteen unknown functions $r_{ij}(t)$, which has to be solved numerically under the initial conditions.

In the following, we have plotted the change in the stored work, $\Delta W = W_{max}(t) - W_{max}(0)$, in units of ω_0 , as a function $\omega_0 t$ for $T = 0$ in Fig.3, where the initial state is chosen as $|\varphi_{AB}(0)\rangle = |1\rangle \otimes |0\rangle$ that the QB is empty. Solid blue line indicates overdamped regime and dashed red line presents underdamped regime that both of them are shown local Markovian dynamics. While dotted purple line remarks overdamped regime and solid green line displays underdamped regime which are considered for local non-Markovian dynamics. As can be seen, the maximum value of stored work, i.e., $\Delta W = \omega_0$, can be provided for underdamped and non-Markovian regime.

In Fig.4, charging power of the battery \mathbb{P} and the upper bound $\sigma_{\mathcal{A}} \sqrt{I_Q}$ are plotted as a function $\omega_0 t$ for $T = 0$. Dashed black line presents $\sigma_{\mathcal{A}} \sqrt{I_Q}$ and red solid line shows \mathbb{P} . Local Markovian dynamics for overdamped and underdamped regime is shown in Fig.4(a) and Fig.4(b) respectively. Also, local non-Markovian dynamics for overdamped and underdamped regime is illustrated in Fig.4 (c) and Fig.4(d), respectively. Numerical results in panels (a)-(d) have been obtained by setting the parameters as Fig.3.

As one can observe, it is clear from Fig.4(d) the greatest

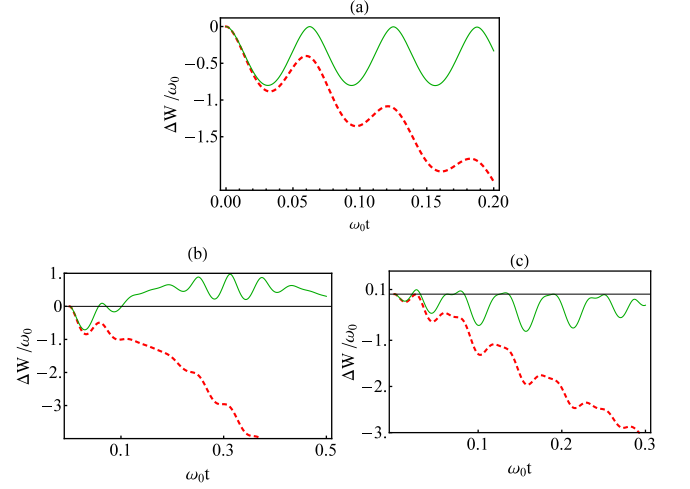


FIG. 6: Panel (a) $|\varphi_{AB}(0)\rangle = \frac{1}{\sqrt{2}}(|0\rangle + |1\rangle) \otimes \frac{1}{\sqrt{2}}(|0\rangle + |1\rangle)$. Panel (b) $|\varphi_{AB}(0)\rangle = \frac{1}{\sqrt{2}}(|0\rangle + |1\rangle) \otimes |0\rangle$. Panel (c) $|\varphi_{AB}(0)\rangle = |1\rangle \otimes \frac{1}{\sqrt{2}}(|0\rangle + |1\rangle)$. Parameters are as Fig.5

value for charging power, $\mathbb{P} = 0.1\omega_0$ can be achieved for underdamped regime and non-Markovian dynamics at the time $\omega_0 t = 15$. Moreover, one can notice that the upper bound, $\sigma_{\mathcal{A}} \sqrt{I_Q}$, at given time intervals, is reached to \mathbb{P} , that implies the bound is saturated.

In order to investigate the role of temperature on the stored work and power, we have plotted ΔW and \mathbb{P} in Fig.5 for $K_B T = 10\omega_0$ and $N = 5$. Additionally, by taking into account the results from Figs.3 and 4, we have regarded only underdamped regime by choosing $\eta = 10\omega_0$ and $\kappa = 50\omega_0$.

Fig.5(a) displays ΔW where dashed red line presents Markovian dynamics and solid green line shows non-Markovian dynamics. As can be observed, in non-Markovian dynamics, the stored work decreases then it becomes growing until reaches to one, then the battery is fully charged at the time $\omega_0 t = 0.3$. Note that the stored work value changes as $-10 \leq \Delta W \leq 1$, where the negative values are due to the temperature and the entropy effects. In addition, regarding Figs.5(b) and (c), we see $\mathbb{P} \simeq 200\omega_0$ for non-Markovian dynamics that is more than the one for Markovian dynamics, also, it is very greater than the case in Fig.4(d).

In the following, let us assume examples showing the effect of initial coherence on the stored work. So, ΔW is depicted for different initial states in Fig.6. We consider the initial state as $|\varphi_{AB}(0)\rangle = \frac{1}{\sqrt{2}}(|0\rangle + |1\rangle) \otimes \frac{1}{\sqrt{2}}(|0\rangle + |1\rangle)$ in Fig.6(a), that there is initial coherence in both of the charger and the battery. Fig.6(a) shows the value of the stored work is always negative and its maximum value is zero, accordingly, the battery can not be charged. We assume $|\varphi_{AB}(0)\rangle = \frac{1}{\sqrt{2}}(|0\rangle + |1\rangle) \otimes |0\rangle$ and $|\varphi_{AB}(0)\rangle = |1\rangle \otimes \frac{1}{\sqrt{2}}(|0\rangle + |1\rangle)$ as initial states in Fig.6(b) and Fig.6(c), respectively. By comparison panel (b) and (c), we see the battery can be charged completely, i.e., $\Delta W = \omega_0$, in the absence of initial coherence in the battery as well as the existence of initial coherence in the charger has no significant effect on the amount of stored work.

VI. CONCLUSION

In this article, we have studied bounds on the charging power of quantum batteries via an open system approach. We have introduced a tighter bound in terms of the variance of activity operator and quantum Fisher information. In addition, we have obtained thermodynamic interpretation of the power and connected to dissipation work and the rate of irreversible entropy.

To confirm the introduced bounds we have investigated two examples. We have first considered the Heisenberg XX spin chain to illustrate the bound is tight. Then, in the second example, we have demonstrated that the battery can be fully

charged in the non-Markovian dynamics and underdamped regime and its power is also greater than the Markovian case. As well as, we have illustrated that charging power increases by increasing the temperature. Moreover, we have shown the existence of initial coherence in the battery has destructive effects on the amount of the stored work.

ACKNOWLEDGMENTS

This work has been supported by the University of Kurdistan. Authors thank Vice Chancellorship of Research and Technology, University of Kurdistan.

-
- [1] S. Deffner and S. Campbell, arXiv:1907.01596 (2019).
 - [2] F. Binder, S. Vinjanampathy, K. Modi and J. Goold, Phys. Rev. E **91**, 032119 (2015).
 - [3] J. Gemmer, M. Michel and G. Mahler, Quantum Thermodynamics, (Springer-Verlag Berlin Heidelberg, 2009).
 - [4] K. Brandner and U. Seifert, Phys. Rev. E **93**, 062134 (2016).
 - [5] J. Goold, M. Huber, A. Riera, L. del Rio and P. Skrzypczyk, J. Phys. A: Math. Theor. **49**, 143001 (2016).
 - [6] S. Vinjanampathy and J. Anders, Contemporary Physics, 57:4, 545 (2016).
 - [7] F. G. S. L. Brandao, M. Horodecki, N. Huei Ying Ng, J. Oppenheim and S. Wehner, PNAS, **112**, 3275(2015).
 - [8] R. Alicki, M. Fannes, Phys. Rev. E **87**, 042123 (2013).
 - [9] F. C. Binder, J. Goold, S. Vinjanampathy, and K. Modi, New J. Phys. **17**, 075015 (2015).
 - [10] F. Campaioli, F. A. Pollock, F. C. Binder, L. Celeri, J. Goold, S. Vinjanampathy, and K. Modi, Phys. Rev. Lett. **118**, 150601 (2017).
 - [11] D. Ferraro, M. Campisi, G. M. Andolina, V. Pellegrini and M. Polini, Phys. Rev. Lett. **120**, 117702 (2018).
 - [12] T. P. Le, J. Levinsen, K. Modi, M. M. Parish, and F. A. Pollock, Phys. Rev. A **97**, 022106 (2018).
 - [13] S. Ghosh, T. Chanda, A. Sen(De), arXiv:1905.12377 (2019).
 - [14] G. M. Andolina, D. Farina, A. Mari, V. Pellegrini, V. Giovannetti, and M. Polini, Phys. Rev. B **98**, 205423 (2018).
 - [15] G. M. Andolina, M. Keck, A. Mari, M. Campisi, V. Giovannetti and M. Polini, Phys. Rev. Lett. **122**, 047702 (2019).
 - [16] K.V. Hovhannisyan, M. Perarnau-Llobet, M. Huber, A. Acín, Phys. Rev. Lett. **111**, 240401 (2013).
 - [17] T. P. Le, J. Levinsen, K. Modi, M. M. Parish, and F. A. Pollock, Phys. Rev. A **97**, 022106 (2018).
 - [18] L. Fusco, M. Paternostro, and G. De Chiara, Phys. Rev. E **94**, 052122 (2016). Y. Y. Zhang, T. R. Yang, L. Fu, and X. Wang, Phys. Rev. E **99**, 052106 (2019).
 - [19] A. C. Santos, B. Çakmak, S. Campbell, and N. T. Zinner, Phys. Rev. E **100**, 032107 (2019).
 - [20] E. Strambini, A. Iorio, y O. Durante, R. Citro, C. Sanz-Fernández, C. Guarcello, I. V. Tokatly, A. Braggio, M. Rocci, N. Ligato, V. Zannier, L. Sorba, F.S. Bergeret, and F. Giazotto, arXiv: 2001.03393 (2020).
 - [21] R. Alicki, arXiv:1903.12140 (2019).
 - [22] D. Rossini, G. M. Andolina, D. Rosa, M. Carrega, and Marco Polini, arXiv:1912.07234(2019).
 - [23] G. M. Andolina, M. Keck, A. Mari, V. Giovannetti, and M. Polini, Phys. Rev. B **99**, 205437 (2019).
 - [24] S. Gherardini, F. Campaioli, Fi. Caruso, and F. C. Binder, arXiv:1910.02458 (2019).
 - [25] A. C. Santos, B. Çakmak, S. Campbell, N. T. Zinner, Phys. Rev. E **100**, 032107 (2019).
 - [26] A. C. Santos, A. Saguia, and M. S. Sarandy, arXiv:1912.03675 (2019).
 - [27] D. Rossini, G. M. Andolina and M. Polini, Phys. Rev. B **100**, 115142 (2019).
 - [28] F. Pirmoradian and K. Mølmer, Phys. Rev. A **100**, 043833 (2019).
 - [29] F. Barra, arXiv: 1902.00422 (2019).
 - [30] J. Q. Quach and W. J. Munro, arXiv: 2002.10044 (2020).
 - [31] F. H. Kamin, F. T. Tabesh, S. Salimi, and F. Kheirandish, arXiv: 1910.07751 (2019).
 - [32] D. Farina, G. M. Andolina, A. Mari, M. Polini, and V. Giovannetti, Phys. Rev. B **99**, 035421 (2019).
 - [33] L. P. G-Pintos, A. Hamma, and A. del Campo, arXiv: 1909.03558 (2019).
 - [34] H.-P. Breuer and F. Petruccione, The Theory of Open Quantum Systems (Oxford University Press, New York, 2002)
 - [35] H. -P. Breuer, E. -M. Laine, J. Piilo, and B. Vacchini, Rev. Mod. Phys. **88**, 021002 (2016).
 - [36] H.-P. Breuer, E.-M. Laine, and J. Piilo, Phys. Rev. Lett. **103**, 210401 (2009); A. Rivas, S. F. Huelga, and M. B. Plenio, Phys. Rev. Lett. **105**, 050403 (2010); S. Luo, S. Fu, and H. Song, Phys. Rev. A **86**, 044101(2012); F. F. Fanchini, G. Karpat, B. Cÿ akmak, L. K. Castelano, G. H. Aguilar, O. J. Faras, S. P. Walborn, P. H. Souto Ribeiro, and M. C. de Oliveira, Phys. Rev. Lett. **112**, 210402 (2014); S. Haseli, G. Karpat, S. Salimi, A. S. Khorashad, F. F. Fanchini, B. Cakmak, G. H. Aguilar, S. P. Walborn, and P. H. Souto Ribeiro, Phys. Rev. A **90**, 052118 (2014); S. Haseli, S. Salimi, and A. S. Khorashad, Quantum Inf. Process **14**, 3581 (2015);
 - [37] S. Julià-Farré, T. Salamon, A. Riera, M. N. Bera, and M. Lewenstein, arXiv:1811.04005 (2019).
 - [38] A. E. Allahverdyan, R. Balian, T.M. Nieuwenhuizen, Europhys. Lett. **67**, 565 (2004).
 - [39] P. Skrzypczyk, A. J. Short, and S. Popescu, Nature Communications **5**, 4185 (2014).
 - [40] F. G. S. L. Brand~ao, M. Horodecki, J. Oppenheim, F. M. Renes, and R. W. Spekkens, Phys. Rev. Lett. **111**, 250404 (2013).
 - [41] D. Braun, G. Adesso, F. Benatti, R. Floreanini, U. Marzolino, M. W. Mitchell and S. Pirandola, Rev. Mod. Phys. **90**, 035006 (2018).

- [42] B. Ahmadi, S. Salimi, A.S. Khorashad, F. Kheirandish, Sci. Rep. **9**, 8746 (2019).
- [43] K. Funo, N. Shiraishi and K. Saito, New J. Phys. **21**, 013006 (2019).
- [44] S. Alipour, and A. T. Rezakhani, Phys. Rev. A **91**, 042104 (2015).
- [45] S. Alipour, A. Chenu, A. T. Rezakhani, A. del Campo, arXiv:1907.07460v1(2019).
- [46] S. Alipour, A. T. Rezakhani, A. Chenu, A. del Campo, and T. Ala-Nissila, arXiv:1912.01939 (2019).
- [47] B. Ahmadi, S. Salimi, A. S. Khorashad, arXiv:1912.01983 (2019).
- [48] F. T. Tabesh, S. Salimi, and A. S. Khorashad, Phys. Rev. A **95**, 052323 (2017).
- [49] J. Liu, H. Yuan, X-M. Lu, and X. Wang, J. Phys. A: Math. Theor. **53**, 023001 (2019). J. Liu, H-N. Xiong, F. Song and X. Wang, Physica. A **410**, 167 (2014).
- [50] H. -P. Breuer, J. Phys. B: At. Mol. Opt. Phys. **45**, 154001 (2012).
- [51] F. T. Tabesh, G. Karpat, S. Maniscalco, S. Salimi, A. S. Khorashad, Quant. Inf. Proc. **17** (4), 87 (2018).